JOURNAL OF GEOPHYSICAL RESEARCH, VOL. 102, NO. D1, PAGES 1355–1370, JANUARY 20, 1997

# The solar cycle variation of total ozone: Dynamical forcing in the lower stratosphere

L. L. Hood
Lunar and Planetary Laboratory, The University of Arizona, Tucson

**Abstract.** Multiple regression methods are applied to estimate the solar cycle variation of (1) zonal mean ozone as a function of altitude and latitude using a combination of Nimbus 7 solar backscattered ultraviolet (SBUV) and National Oceanic and Atmospheric Administration (NOAA) 11 SBUV/2 ozone profile data for a 15-year period; (2) total ozone as a function of latitude, longitude, and season using Nimbus 7 total ozone mapping spectrometer (TOMS) data for a 13.3-year period; (3) lower stratospheric temperature as a function of latitude, longitude, and season using microwave sounding unit (MSU) Channel 4 data for a 16-year period; and (4) lower stratospheric geopotential height as a function of latitude, longitude, and season in the northern hemisphere using Berlin height data for a 30-year period. According to the SBUV-SBUV/2 data, most (about 85%) of the 1.5–2% solar cycle variation of global mean total column ozone occurs in the lower stratosphere (altitudes < 28 km). Evidence is obtained for a related solar cycle variation of lower stratospheric temperature (50-150 mbar) and geopotential height (30, 50, and 100 mbar) with geographic dependences similar to that of the solar cycle variation of total ozone. Specifically, total ozone, lower stratospheric temperature, and lower stratospheric geopotential height have annual mean solar regression coefficients in the northern hemisphere that reach a maximum near 30°N latitude within a longitude sector extending from approximately 160°E to 250°E. Maximum variations from solar minimum to maximum in this sector are approximately 11 Dobson units, 0.8 K near 100 mbar, and 60 m at 50 mbar, respectively. Seasonal solar regression coefficients tend to be statistically significant over larger areas in summer but have larger amplitudes within limited regions in winter. These geographic similarities between total ozone, lower stratospheric temperature, and geopotential height solar coefficients suggest that changes in lower stratospheric dynamics between solar minimum and maximum may play an important role in driving the observed total ozone solar cycle variation. To test this hypothesis, a simplified perturbation ozone transport model is applied to calculate the expected total ozone variation owing to dynamical forcing for the calculated geopotential height solar coefficients, climatological ozone mixing ratios, and zonal winds. For the summer season during which the solar regression coefficients are significant over the largest area, both the amplitude and latitude dependence of the observed solar cycle ozone variation are approximately consistent with the model estimates.

## 1. Introduction

A prerequisite for an accurate determination of anthropogenic trends in ozone is a knowledge of the natural sources of stratospheric interannual variability [e.g., *World Meteorological Organization (WMO)*, 1991, 1995]. While it may be possible in some cases to remove statistically natural variability from a given time series using an appropriate mathematical model, a physical understanding of this variability is also necessary before full confidence in the derived trends will be achieved. Variations occurring on timescales of a few years, associated, for example, with the quasi-biennial oscillation (QBO) and the El Niño-Southern Oscillation (ENSO), are incompletely understood but have relatively minor influences on long-term trend estimates. Variations occurring on decadal and longer timescales are more poorly characterized and can have a more direct impact on trend estimates. Two possible sources of decadal natural variability in the stratosphere are solar variability (occurring mainly on the timescale of the 11-year solar activity cycle) and volcanic emissions [e.g., *Brasseur and Solomon*, 1984]. Because recent major volcanic



Paper number 96JD00210.
0148-0227/97/96JD-00210$09.00

eruptions (especially El Chichon in 1982 and Pinatubo in 1991) have occurred at intervals comparable to the solar cycle length, it is possible that solar and volcanic forcing may be difficult to separate at some latitudes and altitudes (see Figure 10 of *Solomon et al.* [1996] and the accompanying discussion). Hence, further work is needed to evaluate the relative roles of each of these forcing mechanisms in driving stratospheric interannual variability. The present paper is an effort to characterize further the nature and physical origin of the solar component of total ozone variability.

Statistical analyses of ground-based (Dobson and Umkehr) ozone records extending in some cases over more than six decades have previously indicated the occurrence of an in-phase solar cycle variation of global mean total ozone with an amplitude of several per cent from solar minimum to maximum [*Angell*, 1989; *Reinsel et al.*, 1987; *Dütsch et al.*, 1991; *Zerefos et al.*, 1995; R. Bojkov, private communication, 1995]. As discussed, for example, by *Angell* [1989; see his Figures 2 and 3], the correlation of total ozone with solar activity indicators is largest when globally averaged Dobson data are used but is also present within separate geographic zones. Consistent with the ground-based data, recent satellite measurements of global column ozone covering 13 to 15 years have also yielded evidence for an in-phase solar cycle variation with an amplitude of 1.5 to 2% [*Chandra*, 1991; *Hood and McCormack*, 1992; *Chandra and McPeters*, 1994]. While even 60 years of data are insufficient to prove beyond any doubt a causal link between the 11-year solar cycle and total ozone, this interpretation is made plausible by the existence of a number of direct and indirect physical mechanisms by which solar variability could affect ozone in the stratosphere.

Direct solar mechanisms for perturbing ozone include changes in solar ultraviolet spectral irradiance and changes in the flux of precipitating energetic particles [e.g., *Brasseur and Solomon*, 1984]. Although precipitating particles, including highly relativistic galactic protons, energetic solar protons, and relativistic magnetospheric electrons, can significantly perturb upper stratospheric chemistry at high latitudes, the expected effects at lower latitudes are relatively small [*Garcia et al.*, 1984; for a review, see *Jackman*, 1991]. It remains possible that relativistic electron precipitation may be important for the polar odd nitrogen budget with derivative effects at lower latitudes [*Thorne*, 1977; *Baker et al.*, 1987; *Callis et al.*, 1991]. However, the calculated middle atmospheric energy deposition depends sensitively on angular electron flux measurements near geosynchronous orbit and no final consensus on the magnitude of their contribution has yet been reached [*Jackman*, 1995]. Thus there is not yet any definite confirmation of early proposals that the solar cycle variation of stratospheric ozone and temperature may be a direct consequence of particle precipitation effects [*Ruderman and Chamberlain*, 1975; *Crutzen et al.*, 1975; *Zerefos and Crutzen*, 1975].

Solar UV variations at wavelengths less than 242 nm directly modify the rate of photodissociation of molecular oxygen in the upper stratosphere and, hence, the rate of production of ozone. Unlike particle precipitation effects, direct solar UV effects are most pronounced at low and middle latitudes where photolysis rates are greatest. Current estimates for the change in solar UV irradiance near 200 nm from solar minimum to maximum are in the range of 6 to 10% [*Donnelly*, 1991; *Cebula et al.*, 1992; *DeLand and Cebula*, 1993; *Rottman and Woods*, 1995] and also occur on the solar rotation timescale with comparable amplitudes under solar maximum conditions [*Donnelly*, 1991; *London et al.*, 1993].

Observational evidence for the effects of variable solar UV spectral irradiance on upper stratospheric ozone and temperature at low and middle latitudes has been obtained on both the solar rotation timescale [*Gille et al.*, 1984; *Hood*, 1986; *Keating et al.*, 1985; 1987; *Chandra*, 1986; *Hood and Jirikowic*, 1991] and on the solar cycle timescale.

The solar cycle variation of ozone mixing ratio at different levels in the stratosphere has been investigated statistically using 11.5 years of Nimbus 7 solar backscattered ultraviolet (SBUV) data by *Hood et al.* [1993b] and using 15 years of combined SBUV and National Oceanic and Atmospheric Administration (NOAA) 11 SBUV/2 data by *Chandra and McPeters* [1994]. According to these observational studies based on the SBUV and SBUV/2 data, the global mean solar cycle ozone change is a maximum of 4 to 7% near 2 mbar (about 45 km altitude) and decreases rapidly with decreasing altitude to negligibly small values by 6 mbar (about 35 km altitude). In contrast, two-dimensional model calculations employing realistic solar spectral irradiance changes and accounting for temperature feedback effects predict a maximum percentage ozone increase between solar minimum and maximum of 1.5 to 2.5% between 3 and 6 mbar, decreasing to values less than 1.5% below 20 km altitude [*Brasseur*, 1993; *Huang and Brasseur*, 1993; *Fleming et al.*, 1995; *Haigh*, 1994]. A further dilemma arising from the SBUV-SBUV/2 analyses is that the apparent solar cycle variation of the ozone column in the upper and middle stratosphere is much less than what is needed to explain the observed amplitude (1.5 to 2%) of the total ozone solar cycle variation (see section 2). This is also in contrast with two-dimensional model calculations which predict a much larger contribution to the solar cycle total ozone variation in the middle stratosphere than is observed. However, the SBUV-SBUV/2 data are consistent with earlier studies of Umkehr data which found that most of the solar cycle ozone variation occurred near the ozone concentration maximum in the 20 to 30 km altitude range [*Dütsch et al.*, 1991].

As reviewed by *Labitzke and van Loon* [1993, 1995] and *van Loon and Labitzke* [1994], increasing correlative evidence exists for a 10- to 12-year oscillation of lower stratospheric meteorological parameters based on more than 35 years of analyses by the Stratospheric Research Group at the Free University of Berlin. While the time record is still not long enough to unequivocally conclude

that the observed variations are solar forced, this is the leading working hypothesis at present. In particular, a correlation of solar 10.7 cm radio flux (a proxy for long-term solar UV variability) with annually averaged 30 mbar geopotential height has been demonstrated in the northern hemisphere over three and a half cycles. The correlation is a maximum near 30°N and within a broad longitude sector extending from approximately 150°E to 330°E longitude. By geostrophic and thermal wind relationships, the solar-correlated height field variations imply corresponding temperature and wind field differences between solar minimum and maximum. Because the ozone photochemical lifetime is long compared to dynamical timescales in the lower stratosphere, the wind field differences could contribute significantly to the solar cycle variation of total ozone through changes in the rate of ozone dynamical transport.

Although it has not yet been established how changes in solar ultraviolet flux (or other solar-related parameters) can modify lower stratospheric dynamics, some progress in this direction has been made. It was originally speculated by *Hines* [1974] that direct solar-induced changes in upper stratospheric zonal mean dynamics could modify the transmission-reflection properties of upwardly propagating planetary waves, thereby producing indirect dynamical changes in the lower stratosphere and upper troposphere. In the upper stratosphere, it is expected theoretically that solar UV heating and ozone concentration changes between solar minimum and maximum will result in zonal wind perturbations, especially under winter solstice conditions at midlatitudes where the latitudinal gradient of UV heating is a maximum [e.g., *Huang and Brasseur*, 1993; *Hood et al.*, 1993b]. According to present models, the wind increases from solar minimum to maximum are relatively small ($<<$ 5 m/s). Observationally, there is evidence for a zonal wind variation from solar minimum to maximum near the stratopause in December at northern midlatitudes and in June/July at southern midlatitudes [*Kodera and Yamazaki*, 1990; *Hood et al.*, 1993b]. However, the observed stratopause wind variations are much larger in amplitude than expected theoretically (e.g., 23 $\pm$ 9 m/s in December at 1 mbar, 45°N) and are not hemispherically symmetric [*Hood et al.*, 1993b]. It has been argued that this unexpectedly large upper stratospheric wind variation requires a positive feedback due to wave mean flow interactions such that the planetary wave drag on the flow is reduced under solar maximum conditions [*Hood et al.*, 1993b].

As reviewed by *Kodera* [1993], most theoretical investigations of the Hines mechanism applied linear models and obtained little or no evidence for significant effects of upper stratospheric wind field changes on planetary waves at levels below 30 km [*Bates*, 1977, 1980; *Geller and Alpert*, 1980; *Callis et al.*, 1985; *Nigam and Lindzen*, 1989]. However, larger effects at lower stratospheric and upper tropospheric levels have been obtained in (non linear) general circulation model (GCM) experiments [*Boville*, 1984, 1993; *Kodera et al.*, 1990, 1991]. The latter studies suggest that non linear processes in addition to the propagation of planetary waves are capable of producing significant dynamical changes down to tropospheric levels. Recent GCM experiments involving changes in UV input and with a simulated equatorial quasi-biennial oscillation have further indicated that UV-induced changes in the zonal wind field can have dynamical and thermal consequences extending into the lower stratosphere and troposphere [*Balachandran and Rind*, 1995; *Rind and Balachandran*, 1995]. These experiments may ultimately shed light on the issue of why the apparent solar cycle variation of geopotential height in the lower stratosphere is associated with temperature changes in the middle and upper troposphere [*Labitzke and van Loon*, 1995]. However, because the UV forcing employed in the experiments so far was larger than observed over a solar cycle, was independent of wavelength below 300 nm, and no solar cycle variation of ozone was simulated, a direct comparison of the results with observations is not yet possible. It should be noted that a process not included in current GCMs is radiative-photochemical feedbacks on planetary wave propagation. It has been shown analytically that effects of ozone heating on the stability of lower stratospheric waves can be significant [*Nathan et al.*, 1994]. It is therefore possible that these processes combined with the observed solar cycle variation of ozone in the stratosphere may produce secondary feedbacks at lower stratospheric levels that would not be anticipated with existing numerical circulation models.

In this paper a more quantitative understanding of the apparent solar cycle variation of total ozone is sought with the help of several relevant long-term data sets. Of special interest is the question of whether changes in lower stratospheric dynamics (and, hence, ozone advection) from solar minimum to maximum may play a substantial role in driving the solar cycle variation of total ozone. In section 2, a brief review of evidence from SBUV-SBUV/2 data for a solar cycle variation of global mean ozone is presented and the contributions to the total ozone variation from different stratospheric pressure ranges are estimated. In section 3, a multiple regression statistical model is applied to determine the latitude, longitude, and seasonal dependences of the solar regression coefficient for a series of relevant stratospheric quantities. Evidence is obtained for similarities between the geographic dependences of the calculated total ozone solar regression coefficients and those for lower stratospheric geopotential height and temperature. In section 4, a perturbation mechanistic ozone transport model is applied together with the geopotential height solar regression coefficients to estimate the amplitude and latitude dependence of the dynamically forced solar cycle total ozone variation. This model-derived ozone variation is then compared with that derived from the available satellite ozone data to evaluate quantitatively the extent to which dynamical transport changes can account for the observed solar cycle total ozone variation.

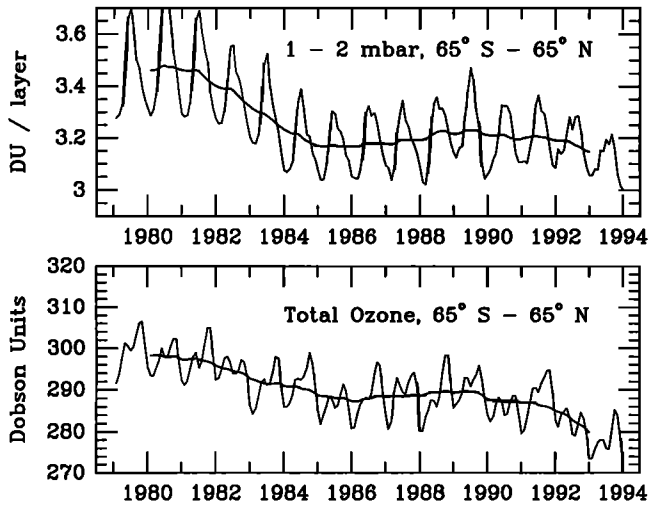


**Figure 1.** (top) A comparison of area-weighted, latitudinal averages of monthly zonal mean SBUV-SBUV/2 ozone in the upper stratosphere and (bottom) for total ozone. Averaging across both hemispheres reduces the amplitude of the annual cycle, allowing long-term variations to be more easily seen. The superposed lines are 25-month running means.

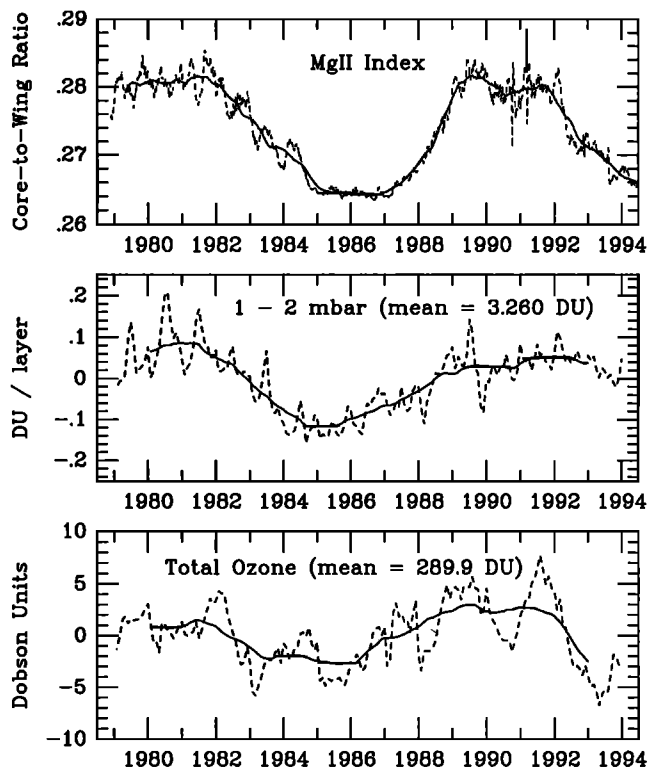


**Figure 2.** (bottom) The dashed lines represent the same data as shown in Figure 1 after deseasonalizing and removing the linear trend. The superposed solid lines are again 25-month running means. (top) The dashed line shows the monthly mean Mg II core-to-wing ratio, a close proxy for solar ultraviolet spectral irradiance near 200 nm (L. Puga, private communication, 1994). (top) The solid line is a 13-month running mean.

## 2. Vertical Distribution of the Total Ozone Variation

In this section a combination of monthly zonal mean Version 6 Nimbus 7 SBUV data [e.g., *McPeters et al.*, 1984] and NOAA 11 SBUV/2 data [e.g., *Planet et al.*, 1994] is considered for the period extending from January 1979 to December 1993. The data consist of estimates for the ozone column abundance within specified pressure layers (Umkehr layers) and have a vertical resolution of approximately 8 km. Useful measurements of the ozone mixing ratio are limited to pressures between approximately 16 and 1 mbar (about 28 to 48 km altitude). The lowermost level at which useful measurements are obtained is limited by the spread of the ozone sensitivity function below the ozone maximum. SBUV measurements at 30 mbar, for example, are more representative of ozone variations in the lower stratosphere as a whole (i.e., total ozone) and do not compare favorably with independent ozone mixing ratio measurements at this level (S. Chandra, private communication, 1995). The amplitude of changes in the ozone column at lower levels (pressures greater than about 16 mbar) is estimated here by taking the difference between the independently measured total ozone change and the measured ozone profile changes at higher levels. For discussions of data quality, long-term stability, and methods used to combine the two separate satellite records, the reader is referred to the papers by *Chandra and McPeters* [1994], *Hood et al.* [1993a], and J. McCormack and L. Hood, *Apparent solar cycle variations of upper stratospheric ozone and temperature: Latitude and seasonal dependences*, submitted to *Journal of Geophysical Research*, 1996.

A comparison between area-weighted, latitudinal averages of monthly zonal mean SBUV-SBUV/2 ozone in the upper stratosphere and total ozone is shown in Figure 1. The upper stratospheric ozone measurements are for Umkehr layer 9 (1 to 2 mbar) and are in units of Dobson units (DU) per layer (1 DU = 1 milliatmosphere centimeter = $2.687 \times 10^{16}$ ozone mol per $cm^2$). A long-term decline in both data records is apparent; however, the decline is not monotonic. A period of relatively rapid decline during the early 1980s is followed by a period of little change during the late 1980s and by an apparent resumption of more rapid decline during the early 1990s. This variation of both upper stratospheric ozone and total ozone has been interpreted as a superposition of a solar cycle variation and a long-term, approximately linear, negative trend [e.g., *Stolarski et al.*, 1991; *Chandra*, 1991; *Hood and McCormack*, 1992; *Hood et al.*, 1993a,b; *Chandra and McPeters*, 1994]. Removing a linear trend and deseasonalizing the data of Figure 1, the time series indicated by the dashed lines in the lower panels of Figure 2 is obtained (see also Figure 3a of *Chandra and McPeters* [1994]). The solid lines in the two lower panels represent 25-month running means, intended to minimize the influence of the quasi-biennial oscillation. The top panel of Figure 2 is a time series representation of the Mg II core-to-wing ratio, a good proxy for solar UV flux at wavelengths

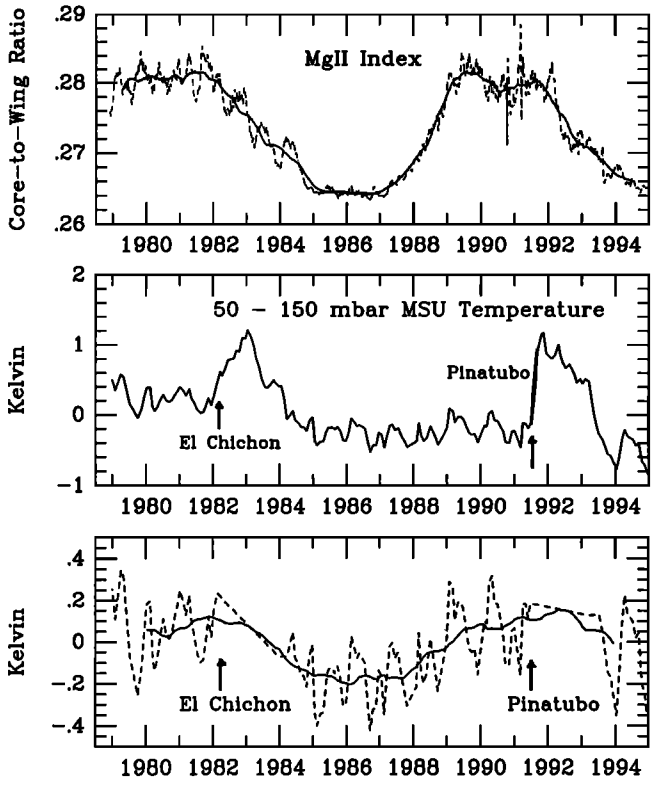


**Figure 3.** (middle) The data is a global mean, deseasonalized temperature deviation for the 50 − 150 mbar layer (maximum weighting near 90 mbar) as derived from channel 4 radiances of the Microwave Sounding Units (MSU) on the NOAA operational satellites [*Spencer and Christy*, 1993]. The times of the El Chichon and Pinatubo volcanic eruptions are indicated. (bottom) The dashed line shows the MSU channel 4 deviation data after removing a linear trend and interpolating linearly across the periods of enhanced temperatures following El Chichon and Pinatubo. (top) Here it is identical to that of Figure 2.

near 200 nm that are important for ozone production [*Heath and Schlesinger*, 1986; *Donnelly*, 1991; *Cebula et al.*, 1992; *DeLand and Cebula*, 1993]. The upper stratospheric ozone and total ozone residuals both vary approximately in phase with the solar UV variation during the 15-year interval for which global data are available. Although the data of Figure 2 suggest that ozone starts to increase before the Mg II index following the 1985-1986 solar minimum, a much longer time series would be needed to establish that a significant phase difference exists. It is more likely that interannual variability associated with the QBO, ENSO, and volcanic eruptions acted to shift the observed ozone minimum forward in time during this particular solar cycle. The amplitude of the global mean total ozone variation from solar minimum to maximum is 1.5 to 2%, in approximate agreement with previous multiple regression studies of the satellite ozone data and with earlier analyses of ground-based Dobson data extending over more than 3 solar cycles [*Angell*, 1989; *Reinsel et al.*, 1987; *Zerefos et al.*, 1996].

Given that the residual global mean total ozone variation shown in the bottom panel of Figure 2 is consistent with that of upper stratospheric ozone shown in the center panel and is consistent with earlier analyses of previous solar cycles using Dobson data, it may be suggested that this variation is physically associated with solar variability. However, as many as 10 additional cycles of data may be required to prove this association in a statistically rigorous sense.

Table 1 lists the results of an approximate calculation of the contributions to the apparent solar cycle total ozone variation from different stratospheric pressure ranges based on the SBUV-SBUV/2 data. Since the SBUV-SBUV/2 data are provided as monthly zonal mean column amounts within Umkehr layers (R. McPeters, private communication, 1995), this calculation is

**Table 1.** Contributions to Solar Cycle Total Ozone Change from Different Stratospheric Pressure Ranges

| Millibars | Dobson Units | Total Dobson Units | Total Percent |
|---|---|---|---|
| | *Upper Stratosphere* | | |
| 0.5 - 1 mbar | 4% × 0.92 DU | = 0.04 DU | |
| 1 - 2 mbar | 4% × 3.3 DU | = 0.13 DU | |
| 2 - 4 mbar | 3% × 10.4 DU | = 0.31 DU | 12% |
| | *Middle Stratosphere* | | |
| 4 - 8 mbar | 3% × 25.2 DU | = 0.13 DU | |
| 8 - 16 mbar | 0% × 47.7 DU | = 0 DU | 3% |
| | *Lower Stratosphere* | | |
| 16 - 32 mbar | 1.5% × 70.2 DU | = 1.05 DU | |
| > 32 mbar | 2.0% × 136.2 DU | = 2.7 DU | 85% |
| Global Mean Solar Cycle Total Ozone Change ≃ 1.5% × 295 DU = 4.4 DU | | | |

straightforward. As reported previously [*Stolarski et al.*, 1991; *Chandra*, 1991], the global mean total ozone variation from solar minimum to maximum was approximately 1.5% during the last cycle, or about 4.4 DU for a global mean ozone value of 295 DU. The largest percentage solar cycle variation of ozone is known to occur in the upper stratosphere and amounts to as much as 4 to 7% [*Hood et al.*, 1993b; *Chandra and McPeters*, 1994]. However, owing to the relatively small ozone column amounts in the upper stratosphere above 4 mbar, the net contribution of the upper stratospheric variation to the total ozone variation is only about 12%. In the middle stratosphere, the ozone column amounts increase substantially but the derived solar cycle variation in this pressure range (4 to 16 mbar) is very small (< 0.5%) leading to a net contribution to the total ozone solar cycle variation of only about 3%. Finally, in the lower stratosphere, the percentage changes of ozone increase somewhat to 1.5-2.0% and the ozone column amounts increase as well. Consequently, a majority (about 85%) of the observed global mean total ozone variation can be attributed to ozone changes occurring in the lower stratosphere (altitudes less than about 28 km).

As discussed in the Introduction, the conclusion that most ($\simeq$ 85%) of the solar cycle variation of total column ozone occurs in the lower stratosphere is at variance with the predictions of current two-dimensional models of the middle atmosphere. Although most models predict a solar cycle total ozone variation of several percent, in approximate agreement with observations, this agreement for total ozone is somewhat misleading. Recent calculations for realistic solar spectral irradiance changes, including the effects of temperature feedback on ozone photochemistry, by *Brasseur* [1993], *Huang and Brasseur* [1993], *Fleming et al.* [1995], and *Haigh* [1994] all predict a maximum percentage ozone mixing ratio increase of 1.5 to 2.5% between solar minimum and maximum in the middle stratosphere (approximately 30 to 40 km altitude). Consequently, these models predict that a relatively large contribution to the ozone column change between solar minimum and maximum occurs in the middle stratosphere (more than 30%) while the contribution in the lower stratosphere is less than 50%. This prediction contrasts with the results of Table 1 which show nearly no contribution from the middle stratosphere and a large majority contribution from the lower stratosphere.

## 3. Statistical Analysis of the Lower Stratospheric Variation

Given the evidence presented above that a large majority of the apparent solar cycle variation of total ozone occurs in the lower stratosphere, it is of interest to investigate statistically the characteristics of this variation and whether there is a corresponding variation of other relevant lower stratospheric physical quantities (temperature, geopotential height). As discussed in the Introduction, evidence has previously been obtained for a 10- to 12-year oscillation of lower stratospheric geopotential height and temperature using analyses carried out at the Free University of Berlin (available only for the northern hemisphere) [*Labitzke and van Loon*, 1993, 1995; *van Loon and Labitzke*, 1994]. To provide an independent assessment, we consider first in this section a global lower stratospheric temperature record with especially good long-term stability. This is the 50-150 mbar weighted mean lower stratospheric temperature time series provided by Channel 4 of the microwave sounding units (MSU) on the NOAA operational satellites [*Spencer and Christy*, 1993; see also *Randel and Cobb*, 1994]. The middle panel of Figure 3 shows the MSU data over a 16-year time period in the form of a global mean, deseasonalized temperature deviation [see, e.g., *Climate Diagnostics Bulletin*, 1995]. Major positive temperature deviations occur in association with the injection of volcanic aerosols following the El Chichon and Pinatubo eruptions. However, a long-term variation is also present that is similar to the total ozone variation in the bottom panel of Figure 1. Specifically, there is a relatively rapid interannual temperature decrease during the early 1980s followed by a period of minimal temperature change or a slight increase during the late 1980s and evidence for a more rapid temperature decrease following the Pinatubo deviation in 1993 and 1994. In the bottom panel of Figure 3, the same data are shown after removing a linear trend and interpolating across the two volcanic episodes. (In both episodes, the volcanically perturbed interval is assumed to be 2 years in length.) An apparent solar cycle variation with a global mean amplitude of 0.2 to 0.3 Kelvin from minimum to maximum is present.

In the remainder of this section, the apparent lower stratospheric solar cycle variation is characterized further by analyzing statistically a series of relevant data sets. Specifically, multiple regression methods will be applied to estimate the latitude, longitude, and seasonal dependences of the solar component of total ozone, lower stratospheric temperature, and lower stratospheric geopotential height variability. In the case of ozone, we consider both zonal mean Version 6 SBUV-SBUV/2 total ozone data (described in the previous section) and Nimbus 7 Total Ozone Mapping Spectrometer (TOMS) data for the period October 1978 to December 1991. The version 6 GRIDTOMS data set is on a 1° latitude by 1.25° longitude grid and has been adjusted for calibration drift to within $\pm$ 1.3% ($2\sigma$) over the 13.3-year measurement period considered here [*Herman et al.*, 1991]. To determine the lower stratospheric temperature regression coefficients, we again analyze the MSU channel 4 data for the 50 to 150 mbar layer with maximum weighting at approximately 90 mbar [*Spencer and Christy*, 1993]. The MSU data are on a 10° longitude by 5° latitude grid and cover the period from January 1979 to December 1994. To determine the lower stratospheric geopotential height regression coefficients, we analyze monthly means of northern hemispheric daily analyses at 30, 50, and 100 mbar on a 5° by 5° grid by the Stratospheric Research Group at the Free University of Berlin [*Pawson et al.*, 1993]. (For some time in-

tervals and levels, these data are only available on a 10° by 10° grid; for these cases, the data were interpolated to 5° resolution.) These height analyses are derived from carefully screened radiosonde data by subjective, nonautomated methods and have relatively good long-term stability. Evidence for both long-term trends and a 10- to 12-year oscillation in the lower stratosphere has previously been derived from the Berlin height analyses [for reviews, see *Pawson et al.*, 1993; *Labitzke and van Loon*, 1993]. The version of the Berlin height data analyzed here covers approximately 30 years from 1964 to 1994 (K. Labitzke, S. Leder, private communication, 1994).

The multiple regression statistical model that is employed here is identical to that used in several earlier studies [*WMO*, 1991; *Stolarski et al.*, 1991; *Hood and McCormack*, 1992; *Hood et al.*, 1993a,b]. It is assumed that the primary components of interannual variability for all analyzed quantities consist of (1) a linear trend describing the stratospheric response to anthropogenic increases in ozone-sensitive trace gases such as chlorine; (2) a quasi-biennial oscillation (QBO) at tropical and extratropical latitudes; and (3) a solar cycle variation. Interannual variability due to volcanic emissions is not explicitly accounted for in the statistical model. These are assumed to be nearly orthogonal to the primary components that are modeled at most latitudes. Specifically, the model is of the form,

$$Y(t) = \mu(i) + \beta_T t + \beta_Q X_{QBO}(t - L) + \beta_S X_{SUN}(t) + \epsilon(t) \quad (1)$$

where $t$ is the time in months; $Y(t)$ represents the monthly mean time series of ozone, temperature, or geopotential height at a given altitude (if applicable), latitude, and longitude; $\mu(i)$ is a seasonal term equal to the long-term mean for the $i$th month of the year ($i = 1, 2, \ldots 12$); $X_{QBO}(t)$ is a time series representing the tropical quasi-biennial oscillation (QBO); $L$ is the optimum phase lag between $X_{QBO}(t)$ and $Y(t)$; $X_{SUN}$ is a time series representing solar variability (no phase lag is assumed); $\epsilon(t)$ is a residual error term; and $\beta_T$, $\beta_Q$, and $\beta_S$ are the coefficients to be determined by least squares regression. To represent the QBO, the Singapore (2° N) 30 mbar zonal wind (J. Angell, private communication; *Climate Diagnostics Bulletin* [1995]) is used. To represent solar variability, we use the Mg II index (L. Puga, private communication, 1994). Applications of (1) to these stratospheric time series without specifying the error term $\epsilon(t)$ generally yield residuals that are first-order autocorrelated. The error term is therefore modeled as a first-order autoregressive process, that is, $\epsilon(t) = r\epsilon(t-1) + w(t)$, where $w(t)$ is white noise [e.g., *Neter et al.*, 1985].

Figure 4 compares the zonal mean and annually averaged solar regression coefficients as a function of latitude from 65°S to 65°N as calculated from the multiple regression model for both SBUV-SBUV/2 total ozone (15 years) and MSU 50 - 150 mbar temperature (16 years). The regression coefficients are expressed in terms of the change in ozone or temperature from solar minimum to maximum, corresponding to a change in the Mg II index of approximately 0.017 and a change in the 10.7 cm solar radio flux of approximately 130 units. The error bars are two standard deviations in length and indicate 95% confidence limits. Positive coefficients significantly different from zero are obtained at most latitudes. Only at high latitudes in the northern hemisphere do the regression coefficients decrease to insignificant values. In the southern hemisphere, the largest coefficient amplitude for ozone occurs at 65°S while in the northern hemisphere, the largest coefficient amplitude occurs at about 30°N. Both the total ozone and lower stratospheric temperature coefficients have a similar dependence on latitude with smaller values near the equator and larger values at approximately 30° latitude in both hemispheres.

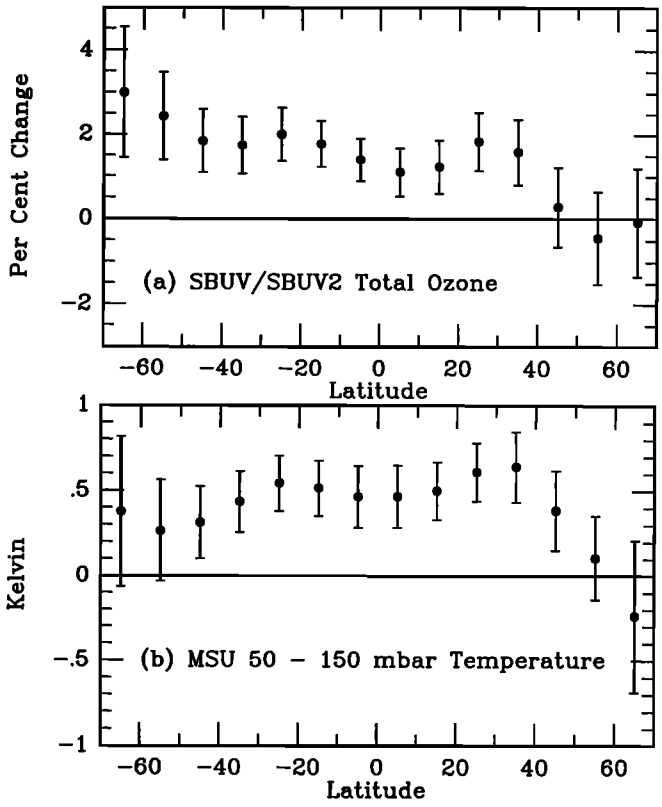


**Figure 4.** Zonal mean and annually averaged solar regression coefficients for (a) SBUV-SBUV/2 total ozone and (b) MSU channel 4 temperature. The error bars represent 2 standard deviations from the mean as calculated from the multiple regression model. In both cases, the regression coefficients are expressed in terms of the change from solar minimum to maximum. In the northern hemisphere, both the total ozone and lower stratospheric temperature solar regression coefficients reach a peak near 30° N and decrease rapidly at higher latitudes.

In the remainder of this section, the longitude, latitude, and seasonal dependences of the solar regression coefficients are examined in the northern hemisphere for which Berlin geopotential height data are available

over a 30-year period. Plate 1 compares the annually averaged solar regression coefficient in the northern hemisphere as derived from 13 years of Nimbus 7 TOMS data (Plate 1a) and from 13 years of simultaneous MSU channel 4 temperature data (Plate 1b). Both data sets analyzed for this figure extend from January 1979 to December 1991 so that a one-to-one comparison is possible. Heavy dark lines divide regions that are statistically significant at the $2\sigma$ level from those that are not. For both ozone and temperature, the 95% confidence level is exceeded only at latitudes less than approximately 45°N, consistent with the zonal mean results of Figure 4. While the largest solar coefficients are obtained near 30°N, as expected from the zonal mean results of Figure 4, the coefficient amplitudes are not longitudinally symmetric. The largest TOMS solar coefficients tend to occur in the 170°E to 230°E sector and there is a corresponding maximum for the MSU solar coefficients in the same sector. Additional TOMS and MSU maxima of smaller amplitude occur in the 0°E to 90°E sector.

Plate 2 shows the annually averaged Berlin geopotential height solar regression coefficient at two levels (30 and 50 mbar) for comparison to the TOMS and MSU coefficients of Plate 1. The entire 30 years of available height data were used to produce Plate 2; however, the results do not change substantially when only the 13-year period covered by the TOMS and MSU analyses of Plate 1 is analyzed. Similar to the TOMS and MSU coefficients, the height solar coefficients at 30 and 50 mbar reach a maximum near 30° or 40°N and become insignificant at latitudes northward of 50°N. Moreover, the height solar coefficients are larger in the 170°E to 270°E sector and maximize near 180°E where the TOMS solar coefficient of Figure 5a is a maximum.

Plates 3 and 4 give an indication of how the TOMS ozone and Berlin 50 mbar height solar coefficients depend on season. Plate 3 compares the TOMS coefficients with the 50 mbar height coefficients for boreal summer. To produce this figure, the TOMS and Berlin height data were first averaged for June, July, and August (JJA) resulting in time series at each latitude and longitude consisting of 13 data points for TOMS and 30 data points for Berlin height. The multiple regression model was then applied using similarly averaged solar and QBO time series. Despite the short record length for TOMS, significantly positive regression coefficients are obtained at low latitudes up to approximately 30°N in most sectors (Plate 3a). The regression coefficient is slightly longitudinally asymmetric with maximum values in the hemisphere centered on 180°E and minimum values near 0°E. For 50 mbar height (Plate 3b), the solar regression coefficient is significantly positive over most of the hemisphere with maximum values near 30° to 40°N in the longitude sector extending from 90°E to 270°E.

Plate 4 shows the result of a similar seasonal regression analysis of the TOMS and Berlin 50 mbar height data for boreal winter (DJF, December, January, and February). In Plate 4a, while most of the hemisphere has relatively small and insignificant solar coefficients, larger and statistically significant values occur near 30°N within certain longitude sectors. The largest coefficients occur near 180°E. Ozone variations during this season are mainly responsible for the coefficient maxima on the annual mean regression map of Plate 1a. The 50 mbar height regression coefficients are also largest near 180°E at northern midlatitudes.

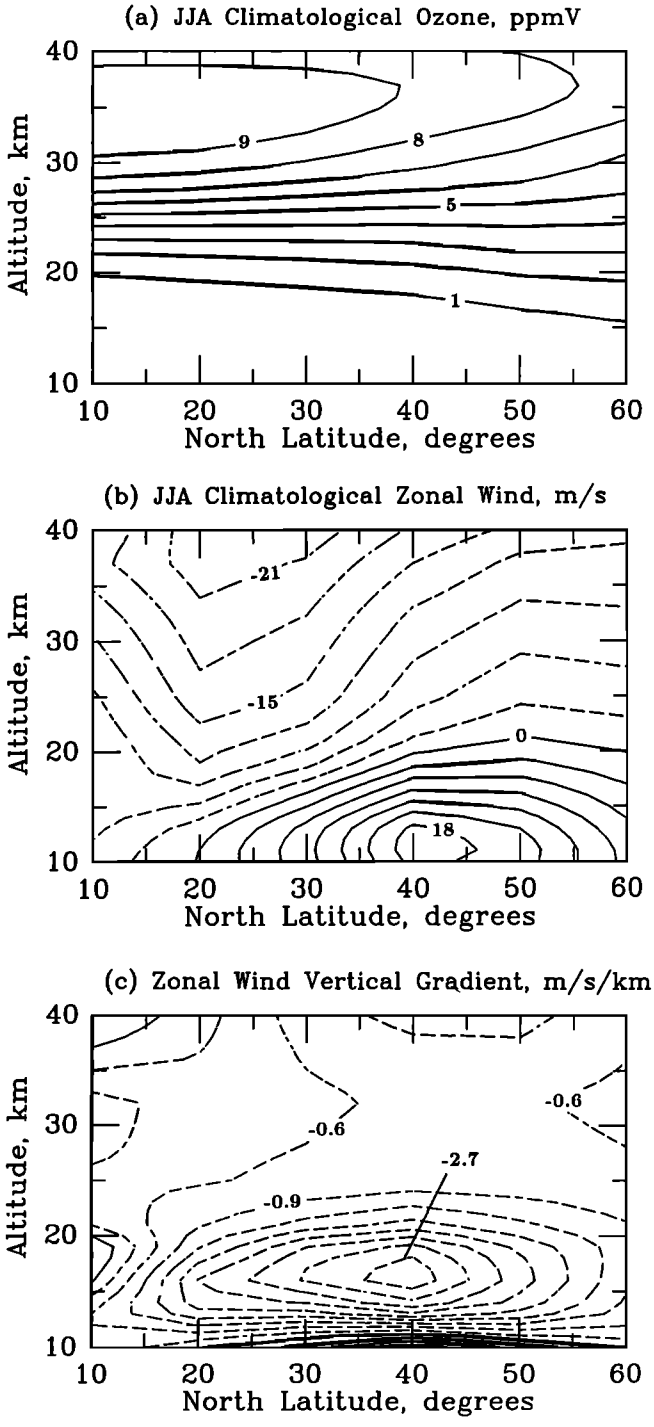


**Figure 5.** (a) Climatological zonal mean ozone mixing ratios (b), zonal winds, and (c) zonal wind vertical gradients, for boreal summer (JJA). See the text for a description of data sources.

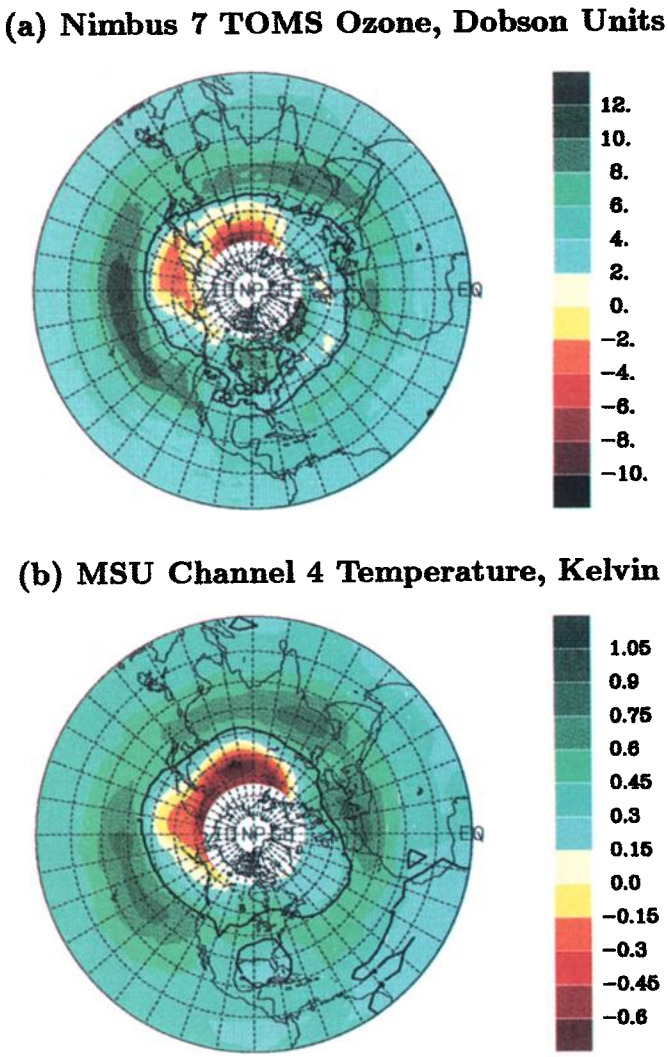


**Plate 1.** Comparison of the annually averaged solar regression coefficients in the northern hemisphere as derived from (a) 13 years of Nimbus 7 TOMS data, and (b) 13 years of simultaneous MSU channel 4 temperature data. The heavy solid line in both plots separates regions where the coefficients are statistically significant at the 2-standard deviation level from regions where the coefficients are not statistically significant. In both cases, coefficients equatorward of 40° to 50° latitude tend to be significantly different from zero.

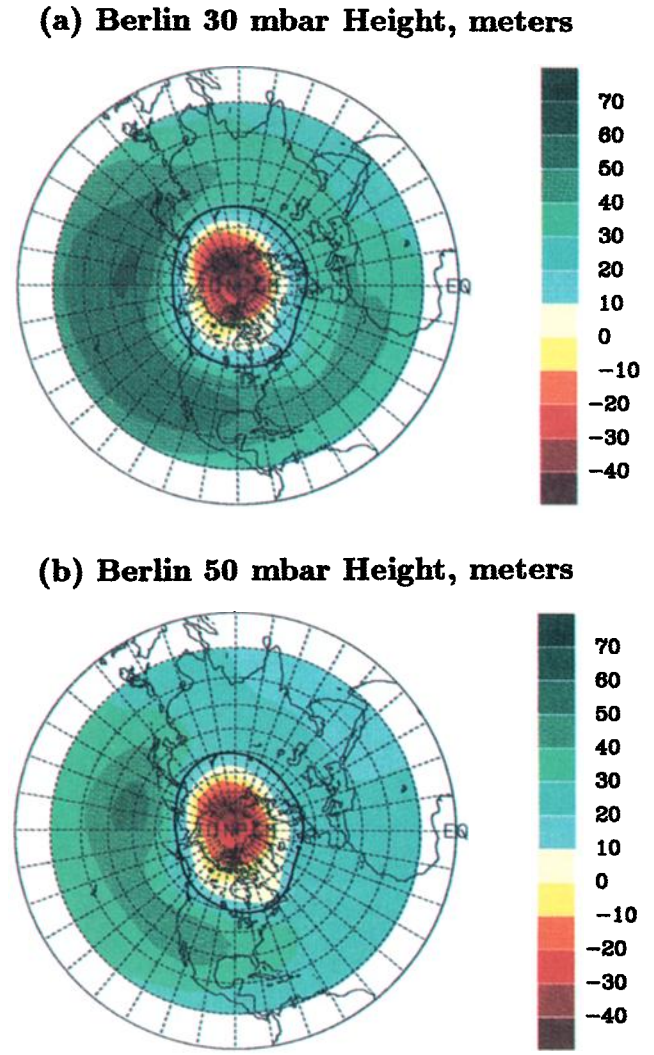


**Plate 2.** Annually averaged geopotential height solar regression coefficients at (a) 30 mbar and (b) 50 mbar as calculated from approximately 30 years of analyses by the Stratospheric Research Group at the Free University of Berlin [*Pawson et al.*, 1993]. The heavy solid lines again separate regions that are not statistically significant from regions that are significant at the $2\sigma$ level. Regions equatorward of 50° to 60° latitude are significant. Results are shown north of 10°N where continuous height data are available.

## 4. Mechanistic Ozone Transport Calculations

The total ozone, lower stratospheric temperature, and lower stratospheric geopotential height solar regression coefficients estimated in the previous section are not easily explained in terms of photochemical and radiative processes alone. Even if only the zonal mean, annually averaged coefficients of Figure 4 are considered, the derived latitude dependence and relative amplitudes of the ozone and temperature regression coefficients are inconsistent with such a model. The latitude dependence of the ozone coefficients (peaking near 30°N and falling off rapidly with increasing latitude in the northern hemisphere; see Figure 4a) is unexpected if only changes in ozone photochemical production rate and constant meridional transport of ozone to higher latitudes are involved. If the ozone coefficients are nevertheless accepted, the associated temperature coefficients are too large to be explained by radiative heating changes alone. This can be confirmed quantitatively by applying a suitable radiative transfer code to calculate approximate bounds on the radiative equilibrium temperature change in the 50-150 mbar layer corresponding

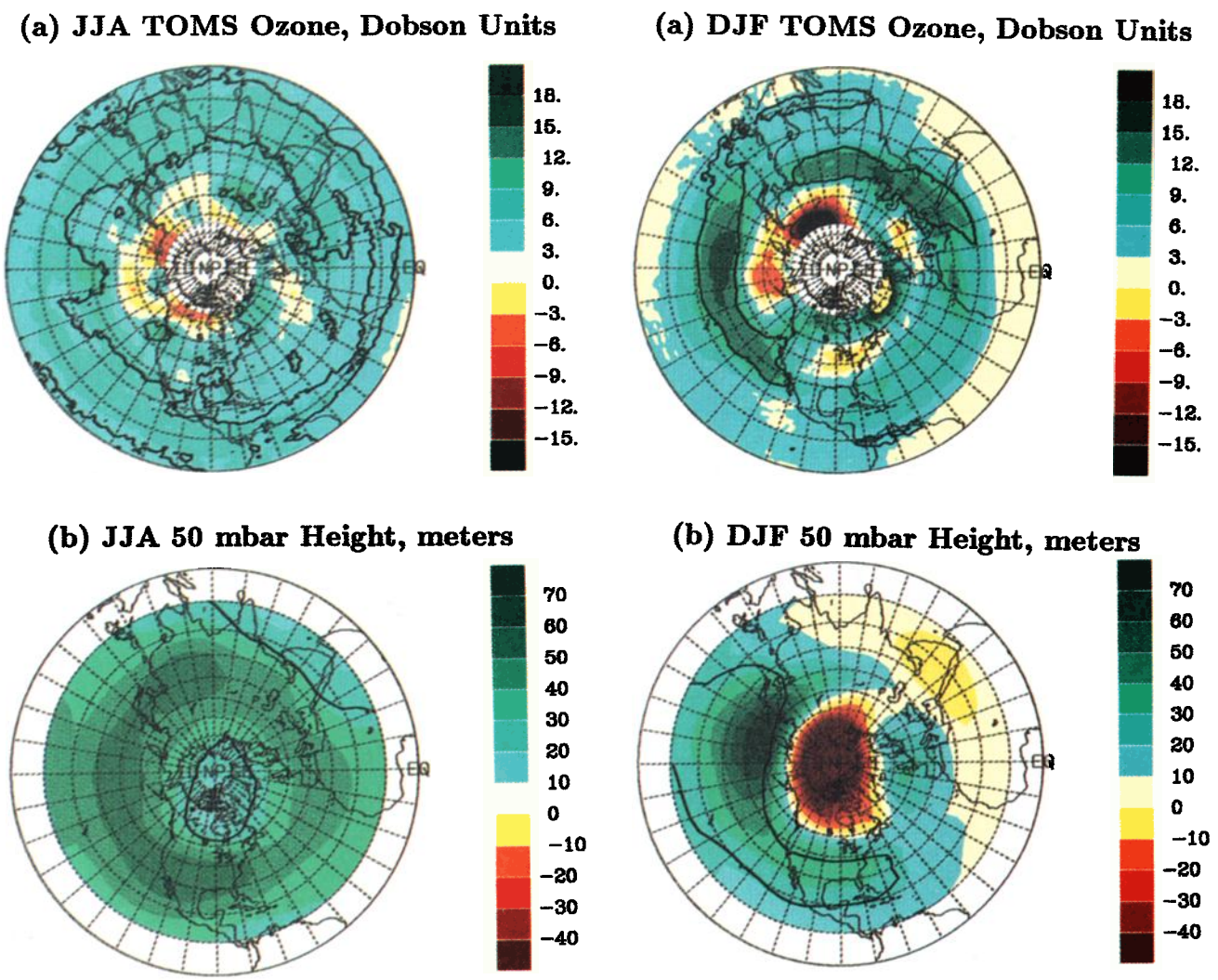


**Plate 3.** Comparison of (a) TOMS ozone and (b) Berlin 50 mbar height solar regression coefficients for boreal summer (JJA). Heavy dark lines again separate zones where coefficients are not statistically significant from zones that are significant at the $2\sigma$ level. On the TOMS plot, regions equatorward of approximately 30° latitude tend to be significant in most longitude sectors.

**Plate 4.** Same format as Figure 7 but for boreal winter (DJF). Note the smaller areal extent of zones that are statistically significant but the higher amplitudes of coefficients within these zones as compared to the results for boreal summer.

to the observed total ozone changes of Figure 4a (J. McCormack, private communication, 1995). The resulting model temperature changes at low latitudes have amplitudes in the range of 0.1 to 0.2 K while the observed temperature changes are of the order of 0.5 K (Figure 4b). Even if uncertainties in the ozone profile change in the lower stratosphere are considered, it is difficult to produce radiative equilibrium temperature changes (in the fixed dynamical heating approximation) significantly greater than 0.2 K.

Given the apparent inadequacy of radiative and photochemical processes, we turn to the hypothesis of dynamical forcing. The similar geographic dependences obtained for total ozone, lower stratospheric temperature, and lower stratospheric geopotential height solar regression coefficients derived in the previous section provide qualitative support for this possibility. For the purpose of a more quantitative investigation, it is useful to consider a mechanistic model for the ozone change in the lower stratosphere due to long-term changes in dynamics alone. In this highly simplified model, photochemistry is neglected in comparison to dynamical advection and it is assumed that the ozone mixing ratio is nearly in a steady state ($\partial/\partial t = 0$). For these assumptions, the ozone chemical continuity equation [*Lindzen and Goody*, 1965; *Andrews et al.*, 1987, p. 414], in perturbation form, reduces to

$$\mathbf{v} \cdot \nabla r \simeq \overline{u}\frac{\partial r'}{\partial x} + v'\frac{\partial \overline{r}}{\partial y} + w'\frac{\partial \overline{r}}{\partial z} = 0. \qquad (2)$$

In (2), $x, y, z$ are Cartesian coordinates in the eastward, northward, and vertical directions, respectively. At a given location, we define the perturbation mixing ratio $r'$ as the deviation from a basic state zonal mean mixing ratio $\overline{r}(y, z)$. Further, we assume that the zonal wind

velocity $u$ is much larger than the meridional ($v$) and vertical ($w$) velocities so that these can be replaced, to first order, by the perturbation quantities $v'$,$w'$ and by $\overline{u}(y, z)$, a basic state zonal mean zonal wind.

Using the geostrophic approximation and applying the perturbation thermodynamic energy equation for an adiabatic process, it is possible to express $v'$ and $w'$ in terms of the geopotential height perturbation $Z'$ on a constant pressure surface as [see, e.g., *Kurzeja*, 1984; *Hood and Zaff*, 1995],

$$v' \simeq \frac{g_o}{f}\frac{\partial Z'}{\partial x} \tag{3}$$

$$w' \simeq \frac{g_o}{N^2}\left(\frac{\partial \overline{u}}{\partial z}\frac{\partial Z'}{\partial x} - \overline{u}\frac{\partial^2 Z'}{\partial x \partial z}\right) \tag{4}$$

where $g_o$ is the mean value of the acceleration of gravity at sea level, $f$ is the Coriolis parameter, and $N^2$ is the buoyancy frequency squared. Here, we have defined $Z'$ as the deviation from a basic state zonal mean geopotential height $\overline{Z}$. Substituting (3) and (4) into (2), multiplying through by $dx$ and integrating, we obtain

$$\Delta r' = -\frac{g_o}{f\overline{u}}\frac{\partial \overline{r}}{\partial y}\Delta Z' - \frac{g_o}{N^2\overline{u}}\frac{\partial \overline{r}}{\partial z}\left(\frac{\partial \overline{u}}{\partial z}\Delta Z' - \overline{u}\frac{\partial}{\partial z}(\Delta Z')\right) \tag{5}$$

where $\Delta r'$ is the approximate change in the ozone mixing ratio resulting from a given change $\Delta Z'$ of the geopotential height. In addition to the quasi-static and photochemically inert assumptions mentioned above, (5) is limited in its applicability to regions away from the equator ($f >> 0$) where $\overline{u}$ does not approach zero ($\overline{u} >> 0$).

In principle, (5) provides a means of estimating the change in ozone mixing ratio at a given level in the lower stratosphere corresponding to a known change in geopotential height from solar minimum to maximum. It is then possible to estimate the corresponding change in the ozone column for comparison with the observational results of section 4. The calculation is complicated somewhat by the large variations of $\overline{u}$, $\overline{r}$, and their gradients with latitude, altitude, and season. As one simplification, we consider here only the boreal summer season (JJA) for which the total ozone solar regression coefficients are statistically significant over the largest area (Plate 3). The analysis is also necessarily restricted to the northern hemisphere where the Berlin height data are available. For the constants in (5), we take values of $g_o = 9.8 \times 10^{-3}$ km s$^{-2}$, $N^2 = 4 \times 10^{-4}$ s$^{-2}$, and $f = (1.454 \times 10^{-4}) \sin\lambda$ s$^{-1}$ where $\lambda$ is latitude. For the basic state quantities, $\overline{r}$ and $\overline{u}$, we adopt the climatological values for boreal summer shown in Figure 5. The basic state ozone volume mixing ratios are based on the data of *Dütsch* [1969] and *Keating and Young* [1985]. The JJA climatological zonal wind values and vertical gradients of Figure 5b and 5c are calculated from National Meteorological Center height data for the years 1979 through 1992 using the gradient wind algorithm [e.g., *Randel*, 1992].

According to Figure 5b, the JJA zonal wind is a strong function of latitude in the lowermost part of the stratosphere. Because $\Delta r'$ is approximately inversely proportional to $\overline{u}$, this leads to a similar strong latitude dependence for the total ozone perturbation resulting from a positive change in geopotential height between solar minimum and maximum. The final model-derived estimates for the JJA zonal mean total ozone variation from solar minimum to maximum are shown in Figure 8 compared to values derived from the TOMS data for the same season.

To illustrate how the model estimates of Figure 8 are obtained, consider two specific latitudes, 20°N and 50°N, where the total ozone perturbation is positive and negative, respectively. Table 2 lists the model parameters leading to these estimates. At 20°N, from the climatological data of Figure 5a, $\partial\overline{r}/\partial y$ is approximately $-3.4\times10^{-5}$, $1.8\times10^{-4}$, and $1.1\times10^{-4}$ ppmV/km at 30, 50, and 100 mbar, respectively. Corresponding values of $\partial\overline{r}/\partial z$ at the same levels are about 0.76, 0.57, and 0.11 ppmV/km. From the data of Figure 5a and 5c we have $\overline{u} \simeq -16.8$, $-13.6$, and $-7.76$ m/s; and $\partial\overline{u}/\partial z \simeq -0.58$, $-0.85$, and $-1.83$ m/s/km, respectively. The geopotential height solar coefficients at 30, 50, and 100 mbar derived from the regression analyses of the previous section are plotted in Figure 6 for both 20°N and 50°N. From the 20°N height data of Figure 6a, $\Delta Z' \simeq 55$, 35, and 20 m. Taking mean altitudes of 24.6, 21.1, and 16.2 km at the three levels, we estimate $\partial(\Delta Z')/\partial z \simeq 6$, 4, and 2.5 m/km, respectively. Substituting the above values into (5), we obtain $\Delta r' \simeq -0.02 + 0.08 = 0.06$ ppmV at 30 mbar, $\Delta r' \simeq 0.09 + 0.02 = 0.11$ ppmV at 50 mbar, and $\Delta r' \simeq 0.07 - 0.01 = 0.06$ ppmV at 100 mbar. These represent increases of 1.3%, 5.9%, and 13.5%, respectively, over the corresponding climatological mixing ratios of 4.2, 2.0, and 0.4 ppmV.

In order to estimate the change in the total ozone column resulting from the calculated mixing ratio increases at 30, 50, and 100 mbar, the climatological zonal mean ozone concentration profile was first approximated by linear interpolation at 1-km intervals between the known values at 1, 2, 5, 7, 10, 30, 50, 100, 300, 400, and 1000 mbar. The solid line in Figure 7a shows the resulting base concentration profile in units of DU/km. To compute this approximate profile, we use the first-order relation [e.g., *Wirth*, 1991], $\epsilon = (114)\gamma\exp(-z/7)$ DU/km, where $\epsilon$ is the concentration in DU/km, $\gamma$ is the mixing ratio in ppmV, and $z$ is altitude in km. The corresponding base total ozone column at 20°N is 283.7 DU. The dashed line in Figure 7a shows the perturbed concentration profile obtained by adding the values of $\Delta r'$ calculated above at 30, 50, and 100 mbar. The corresponding model ozone column is 292.5 DU, representing an increase of 8.8 DU. This is the value plotted at 20°N in Figure 8.

At 50°N, from the climatological data of Figure 5a, values for $\partial\overline{r}/\partial y$ of approximately $-5.5 \times 10^{-5}$, $2.2 \times 10^{-4}$, and $2.3\times10^{-4}$ ppmV/km at 30, 50, and 100 mbar are estimated. Corresponding values for $\partial\overline{r}/\partial z$ are 0.42, 0.48, and 0.20 ppmV/km. From the data of Figure 5b

**Table 2.** Model Parameters at 20°N and 50°N

| P, mbar | $\partial\overline{r}/\partial y$ ppmV/km | $\partial\overline{r}/\partial z$ ppmV/km | $\overline{u}$, m/s | $\partial\overline{u}/\partial z$, m/s/km | $\Delta Z'$, m | $\partial(\Delta Z')/\partial z$, m/km | $\Delta r'$, ppmV |
|---|---|---|---|---|---|---|---|
| 30 | | | | | | | |
| 20°N | −3.4(−5) | 0.76 | −16.8 | −0.58 | 55 | 6.0 | 0.06 |
| 50°N | −5.5(−5) | 0.42 | −3.4 | −0.70 | 50 | 2.4 | −0.16 |
| 50 | | | | | | | |
| 20°N | 1.8(−4) | 0.57 | −13.6 | −0.85 | 35 | 4.0 | 0.11 |
| 50°N | 2.2(−4) | 0.48 | 0.2 | −1.2 | 42 | 2.4 | 0.01 |
| 100 | | | | | | | |
| 20°N | 1.1(−4) | 0.11 | −7.8 | −1.8 | 20 | 2.5 | 0.06 |
| 50°N | 2.3(−4) | 0.20 | 8.9 | −2.0 | 34 | 2.4 | −0.02 |

Values in parentheses are powers of 10 by which primary entries are to be multiplied.
P is pressure in millibars.

and 5c, climatological values for $\overline{u}$ are −3.4, 0.2, and 8.9 m/s while values for $\partial\overline{u}/\partial z$ are −0.7, −1.2, and −2 m/s/km at the same respective levels. (Note that the value for $\overline{u}$ is unacceptably small at 50 mbar; for this case, the value for $\overline{u}$ at the next adjacent pressure level of 30 mbar was used.) From the height data of Figure 6b, $\Delta Z' \simeq 50$, 42, and 34 m. The resulting estimates for $\partial(\Delta Z')/\partial z$ are approximately 2.4 m/km at all three levels.

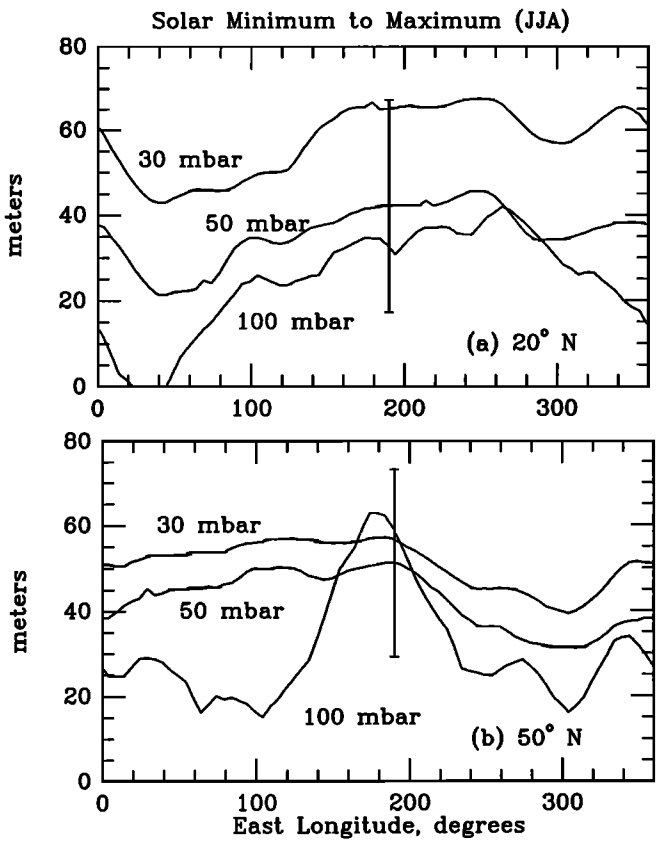


**Figure 6.** Berlin geopotential height solar regression coefficients for three lower stratospheric pressure levels at (a) 20° N and (b) 50° N latitude. The error bars indicate 2 standard deviation uncertainties for the coefficients at 50 mbar and at 190° E. longitude.

Substituting the above values into (5) we obtain $\Delta r' \simeq -0.07 - 0.09 = -0.16$ ppmV at 30 mbar, $\Delta r' \simeq -0.24 + 0.25 = 0.01$ ppmV at 50 mbar, and $\Delta r' \simeq -0.07 + 0.05 = -0.02$ ppmV at 100 mbar. These mixing ratio changes represent changes of −4%, 0.4%, and −3% at these levels over the corresponding climatological values of 4.2, 2.8, and 0.9 ppmV, respectively. The solid line in Figure 7b shows the base concentration profile at 50°N in DU/km, while the dashed line is the perturbed profile obtained by adding the values of $\Delta r'$ estimated above. The corresponding base and model ozone columns are 350.0 and 349.5 DU. The difference of −0.5 DU is the value plotted at 50°N in Figure 8.

From a comparison of the above two calculations at 20°N and 50°N, differences between the zonal wind fields as a function of altitude are largely responsible for the decrease in $\Delta r'$ at 50°N relative to that at 20°N. At 60°N, the total ozone perturbation shown in Figure 8 is decidedly negative. This is due to a smaller positive value (3.8 m/s) for $\overline{u}$ at 100 mbar (Figure 5b) which results in a larger negative contribution in the lowermost stratosphere. Although these calculations are simplified and subject to uncertainties, the results are approximately consistent in both amplitude and latitude dependence with the zonal mean TOMS solar regression coefficients.

## 5. Conclusions

On the basis of satellite ozone profile and total ozone data covering a 15-year period, it has been inferred that a large majority of the apparent solar cycle variation of global mean total ozone occurs in the lower stratosphere (pressures > 16 mbar). Multiple regression statistical studies of lower stratospheric temperature and geopotential height data yield evidence for a solar cycle variation of these physical quantities with geographic and seasonal dependences that are similar to those of total ozone. These similarities suggest that changes in

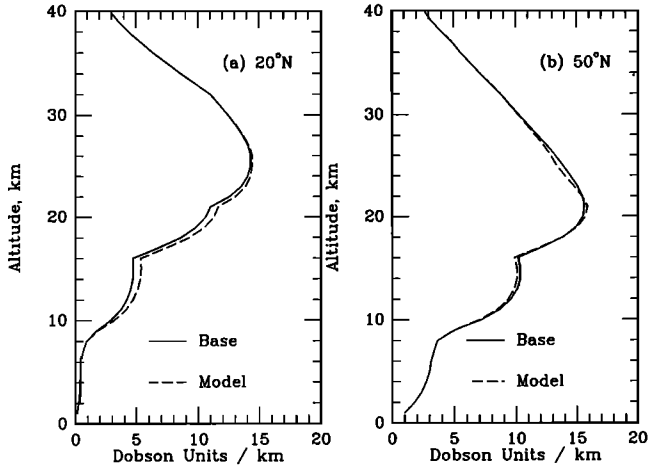


**Figure 7.** The solid lines in both panels represent approximate climatological ozone concentration profiles for solar minimum conditions at (a) 20° N and (b) 50° N latitude for the boreal summer season (JJA). See the text for a description of the computational procedure. The dashed lines in both panels represent perturbed concentration profiles for solar maximum conditions as estimated from the simplified ozone transport model described in the text using the geopotential height solar regression coefficients at 30, 50, and 100 mbar.

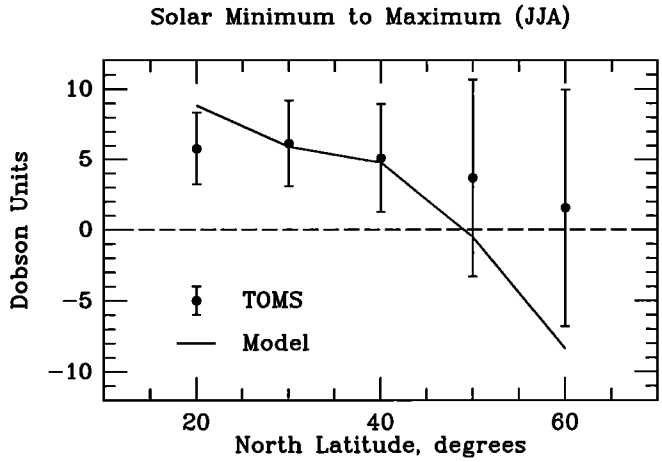


**Figure 8.** Comparison of TOMS zonally averaged solar regression coefficients (points) for boreal summer (JJA) to those estimated from the ozone transport model described in the text using the Berlin height solar regression coefficients (solid line). The error bars on the TOMS coefficients represent two standard deviations from the mean.

mean lower stratospheric dynamics between solar minimum and maximum may contribute substantially to the total ozone variation through changes in the rate of ozone dynamical transport. In section 4, a highly simplified analytic ozone transport model was applied to estimate the ozone mixing ratio perturbations resulting from changes in the geopotential height field at three levels in the lower stratosphere (30, 50, and 100 mbar) where long-term data are available. The analysis was limited to the boreal summer season for which the solar regression coefficients are significant over the largest area and to the northern hemisphere where the Berlin height data are available. Taking into account the latitude dependence of the climatological zonal wind field during this season, it was found that the amplitude and latitude dependence of the observed total ozone variation from solar minimum to maximum could be approximately explained by the transport model. It is therefore concluded that changes in mean ozone dynamical transport in the lower stratosphere are indeed most probably responsible for most of the observed total ozone solar cycle variation. As discussed in the Introduction, these changes in lower stratospheric dynamics are most probably a secondary consequence of the direct effects of solar variability in the upper stratosphere.

It is interesting to note that a previous study of ground-based Dobson total ozone and Umkehr ozone profile data by *Dütsch et al.* [1991] also concluded that the total ozone solar cycle variation at northern midlatitudes is due mainly to variations in ozone transport occurring near the ozone maximum (~ 50 mbar). (Note added in review: Following completion of this paper, it was learned that a recent analysis by *Wang et al.* [1996] of reprocessed Stratospheric Aerosol and Gas Experiment data has confirmed that most of the observed total ozone solar cycle variation occurs just below the ozone concentration peak in the lower stratosphere.) Without additional data, it was not possible in that study to determine whether the solar cycle ozone variation in this altitude range was due to changes in stratospheric circulation or in photochemistry in the tropical source region or both. On the basis of the regression results in section 3 and the calculations in section 4, it appears most probable that changes in stratospheric circulation are dominantly responsible. Unfortunately, as discussed in the Introduction, a full understanding of how the direct upper stratospheric effects of solar variability can indirectly perturb lower stratospheric and upper tropospheric dynamics has not yet been achieved. A more complete understanding of these processes is needed before it can be claimed that the solar cycle variation of total ozone is well understood.

Note added in review: A recent study by *Labitzke and van Loon* [1996] has independently found a geographic similarity between lower stratospheric geopotential height solar correlations and those obtained using TOMS ozone data. They suggest that solar-induced changes in the transport of ozone from the tropics to higher latitudes are responsible for these correlations.

**Acknowledgments.** J. P. McCormack provided assistance in data processing and helped in the interpretation through many valuable discussions. R. D. McPeters and S. Chandra of the NASA Ozone Processing Team at Goddard Space Flight Center kindly transmitted the SBUV-SBUV/2 monthly zonal means and the Nimbus 7 GRIDTOMS data sets analyzed in this paper. M. Jacobs of the Institute of Atmospheric Physics assisted in combining these two data sets and in several aspects of their analysis. The MSU Channel 4 temperatures were provided by J. R. Christy of the

NASA Marshall Space Flight Center; the Mg II core-to-wing ratio values were provided by L. Puga of the NOAA Aeronomy Lab in Boulder, Colorado. Finally, we are especially indebted to K. Labitzke and S. Leder for providing the Berlin geopotential height records utilized in sections 3 and 4. This work is supported by NASA grant NAGW-909 and DOE contract DE-FG03-93ER61727.

## References

Andrews, D. G., J. R. Holton, and C. B. Leovy, *Middle Atmosphere Dynamics*, 489 pp., Academic, San Diego, Calif., 1987.

Angell, J. K., On the relation between atmospheric ozone and sunspot number, *J. Clim.*, *2*, 1404-1416, 1989.

Baker, D., J. Blake, D. Gorney, P. Higbie, R. Klebesadel, and J. King, Highly relativistic magnetospheric electrons: A role in coupling to the middle atmosphere?, *Geophys. Res. Lett.*, *14*, 1027-1030, 1987.

Balachandran, N. K., and D. Rind, Modeling the effects of UV variability and the QBO on the troposphere / stratosphere system, I, The middle atmosphere, *J. Clim.*, in press, 1995.

Bates, J. R., Dynamics of stationary ultra-long waves in middle latitudes, *Q. J. R. Meteorol. Soc.*, *103*, 397-430, 1977.

Bates, J. R., On the interaction between a radiatively damped planetary wave and the zonally averaged circulation in the middle atmosphere, *Pure Appl. Geophys.*, *118*, 266-283, 1980.

Boville, B. A., The influence of the polar night jet on the tropospheric circulation in a GCM, *J. Atmos. Sci.*, *41*, 1132-1142, 1984.

Boville, B. A., The stratosphere in general circulation models, in *The Role of the Stratosphere in Global Change*, edited by M.-L. Chanin, pp. 199-214, Springer-Verlag, New York, 1993.

Brasseur, G., The response of the middle atmosphere to long-term and short-term solar variability: A two-dimensional model, *J. Geophys. Res.*, *98*, 23,079-23,090, 1993.

Brasseur, G., and S. Solomon, *Aeronomy of the Middle Atmosphere*, 441 pp., D. Reidel, Norwell, Mass., 1984.

Callis, L. B., J. C. Alpert, and M. A. Geller, An assessment of thermal, wind, and planetary wave changes in the middle and lower atmosphere due to 11-year UV flux variations, *J. Geophys. Res.*, *90*, 2273-2282, 1985.

Callis, L. B., D. N. Baker, J. B. Blake, J. D. Lambeth, R. E. Boughner, M. Natarajan, R. W. Klebesadel, and D. J. Gorney, Precipitating relativistic electrons: Their long-term effect on stratospheric odd nitrogen levels, *J. Geophys. Res.*, *96*, 2939-2976, 1991.

Cebula, R. P., M. T. DeLand, and B. M. Schlesinger, Estimates of solar variability using the Mg II index from the NOAA-9 satellite, *J. Geophys. Res.*, *97*, 11,613-11,620, 1992.

Chandra, S., The solar and dynamically induced oscillations in the stratosphere, *J. Geophys. Res.*, *91*, 2719-2734, 1986.

Chandra, S., The solar UV related changes in total ozone from a solar rotation to a solar cycle, *Geophys. Res. Lett.*, *18*, 837-840, 1991.

Chandra, S., and R. D. McPeters, The solar cycle variation of ozone in the stratosphere inferred from Nimbus 7 and NOAA 11 satellites, *J. Geophys. Res.*, *99*, 20,665-20,671, 1994.

Crutzen, P. J., I. S. A. Isaksen, and G. C. Reid, Solar proton events: Stratospheric sources of nitric oxide, *Science*, *189*, 457-459, 1975.

DeLand, M., and R. P. Cebula, The composite Mg II solar activity index for solar cycles 21 and 22, *J. Geophys. Res.*, *98*, 12,809-12,823, 1993.

Donnelly, R. F., Solar UV spectral irradiance variations, *J. Geomagn. Geoelect.*, *43*, 835-842, 1991.

Dütsch, H. U., Atmospheric ozone and ultraviolet radiation, *World Survey of Climatology*, vol. 4, edited by D. F. Rex, Elsevier, NY, 1969.

Dütsch, H. U., J. Bader, and J. Staehelin, Separation of solar effects on ozone from anthropogenically produced trends, *J. Geomagn. Geoelectr.*, *43*, 657-665, 1991.

Fleming, E. L., S. Chandra, C. H. Jackman, D. B. Considine, and A. R. Douglass, The middle atmospheric response to short and long term solar UV variations: Analysis of observations and 2D model results, *J. Atmos. Terr. Phys.*, *57*, 333-365, 1995.

Garcia, R., S. Solomon, R. Roble, and D. Rusch, A numerical response of the middle atmosphere to the 11-year solar cycle, *Planet. Space Sci.*, *32*, 411-421, 1984.

Geller, M., and J. Alpert, Planetary wave coupling between the troposphere and the middle atmosphere as a possible sun-weather mechanism, *J. Atmos. Sci.*, *37*, 1197-1215, 1980.

Gille, J. C., C. M. Smythe, and D. F. Heath, Observed ozone response to variations in solar ultraviolet radiation, *Science*, *225*, 315-317, 1984.

Haigh, J. D., The role of stratospheric ozone in modulating the solar radiative forcing of climate, *Nature*, *370*, 544-546, 1994.

Halpert, M. S., and G. D. Bell, eds. *Climate Diagnostics Bulletin*, p.p. 7, National Oceanic and Atmospheric Administration, Washington, D. C., 1995.

Heath, D., and B. Schlesinger, The Mg 280 nm doublet as a monitor of changes in solar ultraviolet irradiance, *J. Geophys. Res.*, *91*, 8672-8682, 1986.

Herman, J. R., R. Hudson, R. McPeters, R. Stolarski, Z. Ahmad, X.-Y. Gu, S. Taylor, and C. Wellemeyer, A new self-calibration method applied to TOMS/SBUV backscattered ultraviolet data to determine long-term global ozone change, *J. Geophys. Res.*, *96*, 7531-7545, 1991.

Hines, C. O., A possible mechanism for the production of sun-weather correlations, *J. Atmos. Sci.*, *31*, 589-591, 1974.

Hood, L. L., Coupled stratospheric ozone and temperature responses to short-term changes in solar ultraviolet flux: An analysis of Nimbus 7 SBUV and SAMS data, *J. Geophys. Res.*, *91*, 5264-5276, 1986.

Hood, L. L., and J. Jirikowic, Stratospheric dynamical effects of solar ultraviolet variations: Evidence from zonal mean ozone and temperature data, *J. Geophys. Res.*, *96*, 7565-7577, 1991.

Hood, L. L., and J. P. McCormack, Components of interannual ozone change based on Nimbus 7 TOMS data, *Geophys. Res. Lett.*, *19*, 2309-2312, 1992.

Hood, L. L., R. D. McPeters, J. P. McCormack, L. Flynn, S. Hollandsworth, and J. Gleason, Altitude dependence of stratospheric ozone trends based on Nimbus 7 SBUV data, *Geophys. Res. Lett.*, *20*, 2667-2670, 1993a.

Hood, L. L., J. Jirikowic, and J. P. McCormack, Quasi-decadal variability of the stratosphere: Influence of long-term solar ultraviolet variations, *J. Atmos. Sci., 50*, 3941-3958, 1993b.

Hood, L., and D. Zaff, Lower stratospheric stationary waves and the longitude dependence of ozone trends in winter, *J. Geophys. Res., 100*, 25,791-25,802, 1995.

Huang, T., and G. Brasseur, Effect of long-term solar variability in a two-dimensional interactive model of the middle atmosphere, *J. Geophys. Res., 98*, 20,413-20,427, 1993.

Jackman, C., Effects of energetic particles on minor constituents of the middle atmosphere, *J. Geomag. Geoelectr., 43*, 637-646, 1991.

Jackman, C., F. M. Vitt, D. B. Considine, and E. Fleming, Energetic particle precipitation effects on stratospheric odd nitrogen and ozone on the solar cycle time scale, IUGG XXI Abstracts, p. B269, paper presented at International Union of Geodesy and Geophysics XXI General Assembly, Boulder, Colo., July, 1995.

Keating, G., G. Brasseur, J. Nicholson III, and A. De Rudder, Detection of the response of ozone in the middle atmosphere to short-term solar ultraviolet variations, *Geophys. Res. Lett., 12*, 449-452, 1985.

Keating, G., J. Nicholson III, D. F. Young, G. Brasseur, and A. De Rudder, Response of middle atmosphere to short-term solar ultraviolet variations, 1, Observations, *J. Geophys. Res., 92*, 889-902, 1987.

Keating, G. M., and D. F. Young, Interim reference models for the middle atmosphere, in *Handbook for Middle Atmosphere Program*, vol. 16, edited by K. Labitzke, J. J. Barnett, and B. Edwards, p. 205-229, Scientific Committee on Solar-Terrestrial Physics, University of Illinois, Urbana, Illinois, 1985.

Kodera, K., Influence of the stratospheric circulation change on the troposphere in the northern hemisphere winter, in *The Role of the Stratosphere in Global Change*, edited by M.-L. Chanin, pp. 227-243, Springer-Verlag, New York, 1993.

Kodera, K., M. Chiba, and K. Shibata, A general circulation model study of the solar and QBO modulation of the stratospheric circulation during the northern hemisphere winter, *Geophys. Res. Lett., 18*, 1209-1212, 1991.

Kodera, K., K. Yamazaki, M. Chiba, and K. Shibata, Downward propagation of upper stratospheric mean zonal wind perturbation to the troposphere, *Geophys. Res. Lett., 17*, 1263-1266, 1990.

Kodera, K., and K. Yamazaki, Long-term variation of upper stratospheric circulation in the northern hemisphere in December, *J. Meteorol. Soc. Jpn., 68*, 101-105, 1990.

Kurzeja, R. J., Spatial variability of total ozone at high latitudes in winter, *J. Atmos. Sci., 41*, 695-697, 1984.

Labitzke, K., and H. van Loon, Some recent studies of probable connections between solar and atmospheric variability, *Ann. Geophys., 11*, 1084-1094, 1993.

Labitzke, K., and H. van Loon, Connection between the troposphere and stratosphere on a decadal scale, *Tellus, 47A*, 275-286, 1995.

Labitzke, K., and H. van Loon, Total ozone and the 11-year sunspot cycle, *J. Atmos. Terr. Phys.*, in press, 1996.

Lindzen, R., and R. Goody, Radiative and photochemical processes in mesospheric dynamics, I, models for radiative and photochemical processes, *J. Atmos. Sci., 22*, 341-348, 1965.

London, J., G. J. Rottman, T. N. Woods, and F. Wu, Time variations of solar UV irradiance as measured by the Solstice (UARS) instrument, *Geophys. Res. Lett., 20*, 1315-1318, 1993.

McPeters, R. D., D. F. Heath, and P. K. Bhartia, Average ozone profiles for 1979 from the Nimbus 7 SBUV instrument, *J. Geophys. Res., 89*, 5199-5214, 1984.

Nathan, T., E. Cordero, and L. Li, Ozone heating and the destabilization of traveling waves during summer, *Geophys. Res. Lett., 21*, 1531-1534, 1994.

Neter, J., W. Wasserman, and M. H. Kutner, *Applied Linear Regression Models*, R. D. Irwin, Homewood, Illinois, 547 pp., 1985.

Nigam, S., and R. Lindzen, The sensitivity of stationary waves to variations in the basic state zonal flow, *J. Atmos. Sci., 46*, 1746-1768, 1989.

Pawson, S., K. Labitzke, R. Lenschow, B. Naujokat, B. Rajewski, M. Wiesner, and R.-C. Wohlfart, *Meteorologische Abhandlungen, Band 7, Heft 3 Climatology of the Northern Hemisphere Stratosphere derived from Berlin Analyses. Part 1: Monthly Means*, 299pp., Verlag von Dietrich Reimer, Berlin, 1993.

Planet, W. G., J. H. Lienesch, A. J. Miller, R. Nagatani, R. D. McPeters, E. Hilsenrath, R. P. Cebula, M. T. DeLand, C. G. Wellemeyer, and K. Horvath, Northern hemisphere total ozone values from 1989-1993 determined with the NOAA-11 Solar Backscatter Ultraviolet (SBUV/2) instrument, *Geophys. Res. Lett., 21*, 205-208, 1994.

Randel, W. J., Global atmospheric circulation statistics, 1000-1 mbar, *NCAR Tech. Note NCAR/TN-366+STR*, 256 pp., Natl. Cent. for Atmos. Res., Boulder, Colo., 1992.

Randel, W. J., and J. B. Cobb, Coherent variations of monthly mean total ozone and lower stratospheric temperature, *J. Geophys. Res., 99*, 5433-5447, 1994.

Reinsel, G. C., G. C. Tiao, A. J. Miller, D. J. Wuebbles, P. S. Connell, C. L. Mateer, and J. J. DeLuisi, Statistical analysis of total ozone and stratospheric Umkehr data for trends and solar cycle relationship, *J. Geophys. Res., 92*, 2201-2209, 1987.

Rind, D., and N. K. Balachandran, Modeling the effects of UV variability and the QBO on the troposphere / stratosphere system, II, The troposphere, *J. Clim.*, in press, 1995.

Rottman, G. J., and T. N. Woods, Solar ultraviolet irradiance: Variation from maximum to minimum of solar cycle 22, IUGG XXI Abstracts, p. B234, paper presented at International Union of Geodesy and Geophysics XXI General Assembly, Boulder, Colo., July, 1995.

Ruderman, M. A., and J. W. Chamberlain, Origin of the sunspot modulation of ozone: Its implications for stratospheric NO injection, *Planet. Space Sci., 23*, 247-268, 1975.

Solomon, S., R. W. Portmann, R. R. Garcia, L. W. Thomason, L. R. Poole, and M. P. McCormick, The role of aerosol trends and variability in anthropogenic ozone depletion at northern midlatitudes, *J. Geophys. Res.*, in press, 1996.

Spencer, R. W., and J. R. Christy, Precision lower stratospheric temperature monitoring with the MSU: Technique, validation, and results 1979-1991, *J. Clim., 6*, 1194-1204, 1993.

Stolarski, R. S., P. Bloomfield, R. D. McPeters, and J. R. Herman, Total ozone trends deduced from Nimbus 7 TOMS data, *Geophys. Res. Lett., 18*, 1015-1018, 1991.

Thorne, R. M., Energetic radiation belt electron precipitation: A natural depletion mechanism for stratospheric ozone, *Science, 195*, 287-289, 1977.

van Loon, H., and K. Labitzke, The 10 - 12 year atmospheric oscillation, *Meteorolog. Zeitschr., N.F., 3*, 259-266, 1994.

Wang, H. J., D. M. Cunnold, and X. Bao, A critical analysis of SAGE ozone trends, *J. Geophys. Res.*, in press, 1996.

Wirth, V., Quasi-stationary planetary waves in total ozone and their correlation with lower stratospheric temperature, Ph. D. thesis, Univ. of Munich, Germany, 1991.

World Meteorology Organization, *Scientific Assessment of Ozone Depletion: 1991*, Global Ozone Research and Monitoring Project, *Rep. No. 25*, WMO Ozone Secretariat, Geneva, Switzerland, 1991.

World Meteorological Organization, *1994 Assessment of $O_3$ Depletion, Rep. 37*, WMO Ozone Secretariat, Geneva, Switzerland, 1995.

Zerefos, C. S., and P. J. Crutzen, Stratospheric thickness variations over the northern hemisphere and their possible relation to solar activity, *J. Geophys. Res., 80*, 5041-5043, 1975.

Zerefos, C. S., K. Tourpalir, B. R. Bojkov, D. S. Balis, B. Rognerund, and I. S. A. Isaksen, Solar activity-total ozone relationships; observations and model studies with heterogeneous chemistry, *J. Geophys. Res.*, in press, 1996.

---

L. L. Hood, University of Arizona, Space Sciences Building, Tucson, AZ 85721. (e-mail:lon@lpl.arizona.edu)

(Received October 2, 1995; revised December 19, 1995; accepted January 11, 1996.)